FULL PAPER

How Well Should the Active Site and the Specific Recognition Be Defined for Proficient Catalysis? – Effective and Cooperative Polyphenol/Catechol Oxidation and Oxidative DNA Cleavage by a Copper(II)-Binding and H-Bonding Copolymer

Vasiliki Lykourinou,[a] Ahmed I. Hanafy,[a,b] Giordano F. Z. da Silva,[a] Kirpal S. Bisht,[a] Randy W. Larsen,[a] Brian T. Livingston,[c] Alexander Angerhofer,[d] and Li-June Ming*[a]

Despite the mainly inhomogeneous and unstructured nature of linear polymers, the Cu^{II} complex of a vinylpyridine-acrylamide copolymer exhibits very efficient 2-electron catalysis toward the oxidation of catechol and derivatives to form quinones with and without 80 mM (0.27 %) H_2O_2, showing remarkable $(0.114–2.67) \times 10^5$ and $(2.83–9.60) \times 10^4$-fold rate enhancements, respectively, in terms of first-order rate constant relative to auto-oxidation of the substrates in an aqueous environment under mild conditions. Metal-binding profiles suggest *the presence of cooperativity* in the catalysis. The oxidation catalysis is inhibited by the di-copper tyrosi-

nase specific kojic acid. Moreover, electron paramagnetic resonance spectra reveal magnetic interaction of the Cu^{II} ions. On the basis of the results, the catalysis by this Cu^{II}-polymer seems to be consistent with the mechanism of type-3 di-copper oxidases. This complex also shows effective single- and double-stranded DNA cleavage in the presence of 1.0 % H_2O_2. These studies suggest this Cu^{II}-polymer complex can serve as a unique "chemical nuclease" and a versatile chemical system for further exploration of Cu–oxygen chemistry.
(© Wiley-VCH Verlag GmbH & Co. KGaA, 69451 Weinheim, Germany, 2008)

Introduction

Most linear polymers are known for their inhomogeneous physical and chemical nature, such as variation in their chain lengths, random sequence in subunit composition of copolymers, disordered polymeric main chains, and flexibility of their side chains. Such inhomogeneous nature renders detailed investigation of their structures very difficult, and mostly impossible for copolymers. Nevertheless, bulk properties of polymers can be quite well controlled, including their hydrophobicity and hydrophilicity, optical, magnetic, and electrochemical properties,[1] and physical shapes, which render their wide applications. Despite the disordered and random sequence in copolymers, a number of metal-binding copolymers have recently been prepared and utilized as catalysts for various metal-centered reactions.[2] A hypothesis can thus be raised that a crystallographically

characterizable active site may not be a key issue in polymer-based catalysis (which nevertheless is not obtainable in polymers). Thus, the question "*How well should the active site and the specific recognition be defined for proficient catalysis?*" in metallopolymers should also be raised which awaits answers in order to further the applications of metallopolymers in catalysis. Since polymers can be easily molded into different physical forms such as films and porous particles, their further applications in heterogeneous catalysis can be envisioned.

The copper-dioxygen chemistry is relevant to the utilization of an oxygen donor, such as O_2 and H_2O_2, in the oxidative transformation of organic molecules by Cu complexes that mimic the action of Cu-containing oxidases.[3,4] These biomimetic chemical systems may be better accessible, more stable, and more catalytically versatile than enzymes, thus may have wider applications and provide chemical insight into the mechanisms of enzymes.[3,4] Although O_2 is readily available in the atmosphere, its use as an oxidation agent in multi-cell organisms requires transportation, storage, and activation specifically carried out by different proteins and enzymes in living organisms.[5] Cu-containing oxygenases,[6] such as tyrosinase and polyphenol oxidase, are ubiquitous. They use O_2 to carry out hydroxylation and/or oxidation reactions. Hydroxylation processes of hydrocarbons to yield alcohols or phenols are spin-forbidden, wherein the paramagnetic triplet-state O_2 needs to

[a] Department of Chemistry, University of South Florida,
4202 Fowler Avenue, Tampa, FL 33620, USA
Fax: +01-813-974-1733
E-mail: ming@shell.cas.usf.edu
[b] Department of Chemistry, Faculty of Science, Al-Azhar University,
Nasr City, Cairo, Egypt
[c] Department of Biology, University of South Florida,
Florida, USA
[d] Department of Chemistry, University of Florida,
Gainesville, FL 32611, Florida, USA

be activated to the singlet state to effectively insert into the singlet C–H bond, and are thus very challenging chemical and industrial tasks. Moreover, copper-based oxidative "artificial nucleases" have received considerable attention owing to their mechanistic flexibility and applications in molecular biology such as DNA footprinting.[7,8] Understanding the activity and mechanism of these Cu-centered chemical systems can provide information about oxidative damage to nucleic acids and other biomolecules and gain better understanding of the mechanisms of copper enzymes,[6,9,10] with possible applications in the fields of environmental green chemistry,[11] aging, cancer research, and oxidative stress-associated apoptosis.[12,13–14]

Design aspects of biomimetic systems rely on the structural features of their biological templates, such as the metal-binding sites in metalloenzymes.[15,16] We previously prepared and investigated a metal-binding copolymer (**P1**) of 4-vinylpyridine (4Vp) and acrylamide (Ac) with an average repeating unit (RU) of 4Vp$_3$Ac$_1$ to further explore the versatility of metallopolymers. **P1** was demonstrated to bind metal ions with a stoichiometry of metal/RU = 1:1.[17] This polymer can bind metal ions through the pyridine ring and potentially form H-bonds with its amide group, and may thus loosely mimic the active-site environment of various metalloenzymes. Despite the poorly defined "active site" in these bio-mimicking metallopolymer complexes, they have been demonstrated to exhibit significant hydrolytic activities.[17] Herein, we reveal the oxidative activity of Cu^{II}-**P1** and discuss its mechanism for the oxidations of polyphenol and catechol and oxidative cleavage of DNA in the presence of the green oxidizing agents, H$_2$O$_2$ and the air, in aqueous environment under mild conditions.

Results and Discussion

Polyphenol/Catechol Oxidation

Although H$_2$O$_2$ is a widely used oxidation reagent, it requires further activation by a catalyst for effective oxidation to take place. For example, the oxidation of the polyphenol 1,2,3-trihydroxybenzene (THB) by H$_2$O$_2$ in an aqueous environment (1:1 methanol/25 mM MES buffer at pH 6.0 and 25 °C) is indeed a very slow process, affording a pseudo-first-order rate constant of $k_o = 3.45 \times 10^{-6}$ s^{-1} for the rate law rate = k_o [H$_2$O$_2$] toward 8 mM THB which represents a half-life ($t_{1/2}$) of 55.8 h. Conversely, THB oxidation by H$_2$O$_2$ is dramatically enhanced by 10 μM RU of Cu^{II}-**P1** under the above conditions which reaches a plateau at high [THB] (Figure 1a). Such kinetic pattern indicates an enzyme-like pre-equilibrium kinetic pathway [i.e., THB = S in Equation (1) and Equation (2); Experimental Section], which also reflects that the polyphenol substrate binds directly to the metal center in Cu^{II}-**P1** to afford the S-Cu^{II}-**P1** intermediate [Equation (1)]. A free-radical-initiated oxidation would not show such pre-equilibrium kinetics and the substrate-bound intermediate, wherein second-order kinetics is expected with much higher reaction rate and less selectivity.[18] On the contrary, such a pre-equilibrium kinetic pattern is

not observed when the metal alone or the metal with the monomers 4Vp and Ac are used as the control under the same conditions.
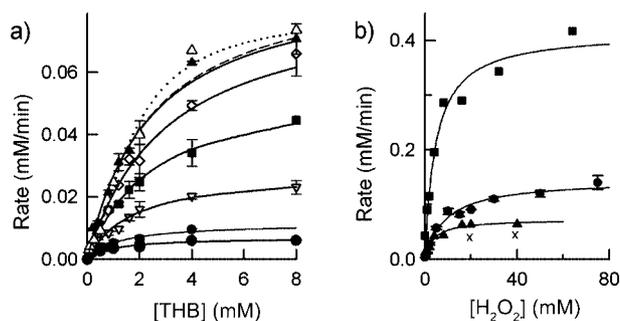

Figure 1. (a) Rate for the oxidation of THB in the presence of 0, 1.0, 2.0, 5.0, 40, and 80 mM H$_2$O$_2$ (from bottom) and the rate ($\times 1/10$) for the oxidation of DTBC in the presence of 50 mM H$_2$O$_2$ (Δ) and fitted with pre-equilibrium kinetics (dashed) and the Hill equation (dotted). (b) Rate for the production of *o*-quinone from 8.0 mM THB (●), 10 mM DTBC (■), and 4 mM catechol (▲) by 10 μM Cu^{II}-**P1**(RU) and a higher concentration (10 mM) of catechol (×) by 10 μM Cu^{II} in the presence of 3 equiv. of 4-Vp and 1 equiv. of Ac. All the experiments were performed in 1:1 methanol/25 mM MES buffer at pH 6.0 and 25 °C.

Fitting the rates of THB oxidation in the presence of 0.27%[19] H$_2$O$_2$ (80 mM) as a function of [THB] to Equation (2) yields a first-order rate constant $k_{cat} = 0.152$ s^{-1} ($t_{1/2} = 4.6$ s), an apparent dissociation constant $K' = 2.40$ mM, and the catalytic efficiency $k_{cat}/K' = 63.3$ M^{-1} s^{-1} (▲; Figure 1a). This catalysis afford a significant rate enhancement of 2.83×10^4-fold in terms of k_{cat}/k_o, i.e., under saturating substrate conditions, wherein the slow background oxidation of THB was determined to give $k_o = 5.38 \times 10^{-6}$ s^{-1} for the rate law rate = k_o [THB]. Despite the structural randomness of copolymers, the results indicate that metallo-active sites in **P1** seem to properly assemble upon Cu^{II} binding to perform this effective oxidative catalysis of THB in the presence of the green oxidation reagent H$_2$O$_2$.

Similar to the polyphenol THB, the commonly used catechol substrate 3,5-di-*tert*-butylcatechol (DTBC) was effectively oxidized by Cu^{II}-**P1** in the presence of 50 mM H$_2$O$_2$ ($\times 1/10$; Δ; Figure 1a). The catalysis follows the same pre-equilibrium kinetics to give $k_{cat} = 1.55$ s^{-1} ($t_{1/2}$ of only 0.447 s), $K' = 2.45$ mM, and $k_{cat}/K' = 633$ M^{-1} s^{-1} (dashed trace; Figure 1a). A considerable first-order catalytic proficiency k_{cat}/k_o of 2.67×10^5-fold was obtained with respect to k_o of 5.80×10^{-6} s^{-1} under the same conditions. There seems to be a slight cooperativity with a Hill coefficient $\theta = 1.56$ (dotted trace) for the oxidation of DTBC; while THB gives a small $\theta = 1.05$. The cooperativity is probably partially due to interactions/influences among metal centers during catalysis (discussed later).

A plot of the rate of oxidation of 8.0 mM THB in aqueous 1:1 methanol/25 mM MES buffer at pH 6.0 and 25 °C by Cu^{II}-**P1** as a function of [H$_2$O$_2$] is also non-linear which can be fitted to Equation (2) to give $k_{cat} = 0.241$ s^{-1}, $K' = 9.70$ mM, and $k_{cat}/K' = 24.8$ M^{-1} s^{-1} (●; Figure 1b) and a

significant rate enhancement of 6.99×10^4-fold in terms of k_{cat}/k_o. Likewise, the oxidation of 10 mM DTBC as a function of $[H_2O_2]$ (■; Figure 1b) yields $k_{cat} = 0.65$ s^{-1}, $K' = 6.58$ mM, and $k_{cat}/K' = 98.8$ M^{-1}s^{-1}, affording 1.1×10^5-fold rate enhancement with respect to $k_o = 5.80 \times 10^{-6}$ s^{-1} for DTBC auto-oxidation. The more inert substrate catechol (4 mM) can also be oxidized into quinone in the presence of H_2O_2, showing $k_{cat} = 0.12$ s^{-1} and $K' = 3.8$ mM (▲; Figure 1b). The rate is higher than the oxidation of catechol at a higher concentration (10 mM) catalyzed by Cu^{II} in the presence of 3 equiv. of 4-Vp and 1 equiv. of Ac (×; Figure 1b). The observation of saturation kinetics herein indicates that H_2O_2 binds to the Cu^{II} center during the oxidative catalyses, following the pathways shown in Equation (1).

A noticeable rate of THB oxidation by 10 μM Cu^{II}-**P1** was detected in the absence of H_2O_2 which was significantly higher than its auto-oxidation rate. Herein, O_2 in the air serves as the oxidation agent which is only 0.27 mM at 25 °C for 100% air saturated water. This aerobic oxidation of THB by Cu^{II}-**P1** also follows pre-equilibrium kinetics [Equation (1), Equation (2)], giving rate constants $k_{cat} = 0.012$ s^{-1} ($t_{1/2} = 58$ s), $K' = 1.02$ mM, and $k_{cat}/K' = 11.8$ M^{-1}s^{-1} (the lowest trace ●, Figure 1a). This catalysis affords 3.12×10^4-fold rate enhancement in terms of k_{cat}/k_o, wherein the auto-oxidation rate constant k_o under the same conditions is 3.85×10^{-7} s^{-1} ($t_{1/2} = 21$ d). Similarly, aerobic oxidation of DTBC by Cu^{II}-**P1** at pH 6.0 yields $k_{cat} = 0.065$ s^{-1} and $K' = 0.16$ mM. The dramatic decrease in the K' value results in a significant catalytic efficiency $k_{cat}/K' = 406$ M^{-1}s^{-1}. The catalysis affords $k_{cat}/k_o = 9.60 \times 10^4$ with k_o determined to be 6.77×10^{-7} s^{-1} under the same conditions, representing a dramatic decrease in $t_{1/2}$ from 11.9 d to 10.7 s. The significant influence of H_2O_2 on K' reflects a mutual exclusion of the two substrates, THB/DTBC and H_2O_2, showing much higher K' values for THB and DTBC in the presence of H_2O_2.

The rate constants in the studies herein are comparable or higher than those of a number of structurally defined Cu^{II} complexes and Fe^{III}-porphyrin systems[20–25] toward the oxidation of catechol and derivatives, and are only ca. 150–350 times lower than that of horseradish peroxidase toward THB oxidation.[25] For example, k_{cat} for the oxidation of catechol is in the range of $(1.6–2.2) \times 10^{-4}$ s^{-1} by Cu^{II}-macrocycle complexes[20] and $(2.75–5.13) \times 10^{-4}$ s^{-1} and $(3.98–13.2) \times 10^{-3}$ s^{-1} by some dinuclear Cu^{II} complexes;[21,22] oxidation of DTBC in methanol or mix solvent by di-Cu^{II} complexes shows $k_{cat} = 0.0553–1.81$ s$^{-1[23,26]}$ and $k_{cat}/K_m = 60–140$ M^{-1}s^{-1};[24] oxidation of THB by the Fe^{III}-heme complex of a catalytic antibody gives $k_{cat} = 0.83$ s^{-1} and $k_{cat}/K_m = 210$ M^{-1}s^{-1} in the presence of 5 mM H_2O_2 at pH 8.0 and $k_{cat} = 42$ s^{-1} and $k_{cat}/K_m = 9100$ M^{-1}s^{-1} by horseradish peroxidase.[25] Moreover, DTBC oxidation by Cu^{II}-**P1** without H_2O_2 shows a significant 1.2% activity relative to that of gypsywort catechol oxidase[27] in terms of the second-order rate constant k_{cat}/K_m.

Because both THB and H_2O_2 can bind to the Cu^{II} center as shown by the pre-equilibrium kinetic pattern [Figure 1a, b; Equation (1)], the catalysis by Cu-**P1** is thus considered

a bi-substrate reaction. The data were analyzed with the Hanes plots [Equation (3), Figure 2a], which are consistent with a random bi-substrate mechanism.[28] The secondary plots from the Hanes plots derived from Figure 1a (i.e., A = THB and B = H_2O_2; Figure 2a) as a function of $1/[H_2O_2]$ according to Equation (3) yield $K'_{THB} = 6.37$ mM, $K'_{H2O2} = 15.4$ mM, and $K'_{iTHB} = 0.76$ mM. The intrinsic dissociation constant K'_{iTHB} is close to the value of 1.02 mM for THB oxidation without H_2O_2, which confirms the validity of this data process according to the bi-substrate mechanism. The K'_{iTHB}/K'_{THB} ratio of 0.12 is much smaller than 1.0 which indicates the binding of H_2O_2 to the active center significantly decreases THB binding affinity to afford a relatively larger K'_{THB} value[28] (i.e., in the case of oxidation of THB in the presence of H_2O_2). A similar Hanes-plot analysis for the rate-vs.-$[H_2O_2]$ plots at various [THB] [i.e., with A and B switched in Equation (3)] yields $K'_{iH2O2}/K'_{H2O2} = 0.103$ (Figure 2b), indicating the binding of THB also decreases H_2O_2 affinity to the metal center, suggesting some exclusive nature of the polyphenol THB and the oxidant H_2O_2 in metal binding.
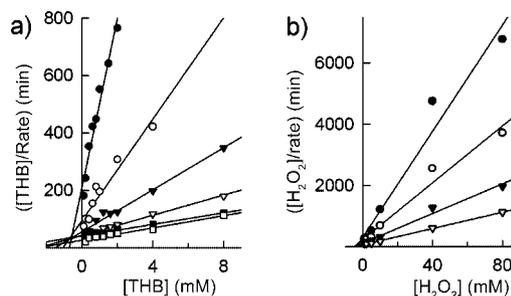

Figure 2. Hanes plot of THB oxidation by Cu^{II}-**P1** in the presence of 0, 1.0, 2.0, 5.0, 40, and 80 mM H_2O_2 (a; from top) and 0.4, 0.8, 2.0, and 4.0 mM THB (b; from top), from which the dissociation constants in Equation (3) can be obtained.

Because cooperativity is an important biological property, possible cooperativity of the metal centers was further investigated, wherein Cu^{II} was added to **P1** in the presence of the redox-inactive Zn^{II} at a constant total concentration of ([Cu^{II}] + [Zn^{II}]) and monitored with the oxidative activity. A proportional increase in the activity with the mol fraction of Cu^{II} (X_{Cu}) should be observed until 1 equiv. of Cu^{II} is added for a simple Cu^{II} binding to the copolymer if there is no cooperativity during catalysis since isolation of Cu^{II} ions from each other by Zn^{II} ions should not affect the activity in this case (dashed fittings, Figure 3). On the contrary, sigmoidal activity profiles were observed toward the oxidation of THB with and without 15 mM H_2O_2, giving Hill coefficients θ of 1.4 and 2.8, respectively (solid fittings, Figure 3). The results suggest a possible presence of cooperativity among Cu^{II} centers for polyphenol oxidation by Cu^{II}-**P1**. This cooperativity may be a consequence of dinuclear catalysis of the 2-electron oxidation of polyphenol and catechol. Herein, Cu^{II} is well isolated by Zn^{II} ions at lower X_{Cu}.
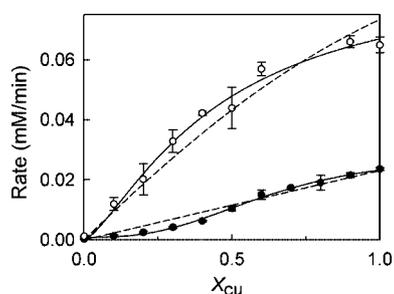
Figure 3. Oxidative activity of Cu-**P1** toward THB in the absence (●) and presence (o) of 15 mM H$_2$O$_2$ as a function of Cu^{II} mol fraction (X$_{Cu}$) at a fixed total concentration of Cu^{II} and Zn^{II}. The traces are fittings to the Hill equation (solid traces) or a simple 1:1 metal-to-ligand binding (dashed traces).

Cooperativity is a common property of multi-domain proteins/enzymes. The presence of catalytic cooperativity was revealed in a recent study of dendrimer-based chemical model system,[29] presumably attributing to the proximity of the active centers on the dendritic arms. Cooperativity of dendrimers toward metal binding has also been previously demonstrated in a few metal-binding dendrimers,[30] showing a distinct difference in metal-binding when the dendritic arms were isolated units. It is worth noting that the simple metallopolymer Cu^{II}-**P1** described herein also exhibits cooperativity in metal binding and catalysis, which is mostly likely attributed to the proximity of the metal centers due to folding of the polymer chains. The observation of cooperativity suggests that metallopolymers can serve as reasonable functional models for metalloenzymes.

The EPR spectrum of Cu^{II}-**P1** under the conditions for the kinetic studies was obtained in the presence of 0.75 equiv. of Zn^{II} per RU for the purpose of magnetic dilution, which shows an axial magnetic environment with $g_\perp$ = 2.270, $g_\perp$ = 2.085, and $A_\perp$ = 553 and $A_\perp$ = 35 MHz (dotted trace; Figure 4a). These values are consistent with those reported for a Cu^{II} center with a nitrogen-rich ligand environment.[31] The spectral features can be attributed to a typical tetragonally distorted Cu^{II} center, i.e., an elongation along the z axis due to the Jahn–Teller effect.
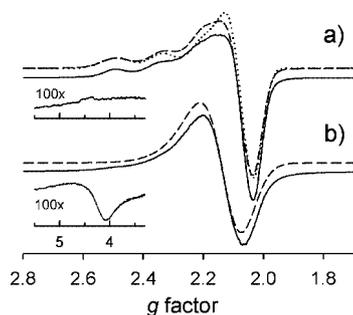

Figure 4. X-band EPR spectra of Cu^{II}-**P1** with (a) and without (b) magnetic dilution by Zn^{II} (75%). The insets are low-field region that show the weak forbidden transition due to magnetic coupling. The dotted trace in (a) is the fitted spectrum for an axial species. While (b) is fitted to show only slight anisotropy (dashed), (a) is best fitted (dashed) as a mixture of 85% of the axial species (dotted) and 15% of the magnetically coupled species (b).

The fitting of the EPR spectrum is not perfect probably because of the presence of magnetically coupled Cu^{II} clusters (see below). The line-broadening in the spectrum suggests the presence of magnetic interactions between/among Cu^{II} ions. When 1 equiv. of Cu^{II} is added to **P1** without Zn^{II} dilution, the spectrum becomes much broader and shows complete loss of the hyperfine features in the $g_\perp$ region (Figure 4b) with a small anisotropy of $g_\perp$ = 2.200, $g_\perp$ = 2.125 and a peak-to-peak width of 200 G, noticeably larger than that in the sample with 75% Zn^{II} dilution (120 G from the simulation; Figure 4a). A weak and broad signal at g = 4.3 in Figure 4b (inset), which is missing in the magnetically diluted sample (inset, Figure 4a), is likely to be attributed to the forbidden |ΔM$_S$| = 2 transition owing to magnetic coupling frequently observed in dinuclear Cu^{II} complexes.[26,32] The Zn^{II}-diluted sample can be better fitted (dashed trace in Figure 4a) by considering the presence of 15% magnetically coupled system from (b). The results indicate that Cu^{II} ions can be close to each other to form magnetically coupled centers in Cu^{II}-**P1**. The proximity of Cu^{II} ions in the polymer can thus result in dinuclear catalysis and cooperativity.

The d–d transition of Cu^{II}-**P1** at 615 nm (Figure 5) reflects a quite strong ligand field, most likely attributing to its all-N ligand environment with a distorted octahedral geometry consistent with the EPR results. For comparison, the all-N(His) ligated Cu^{II}-substituted carbonic anhydrase B absorbs at 750 nm with $g_\perp$ = 2.31 and $g_\perp$ = 2.06[33] and Cu,Zn-superoxide dismutase absorbs at 680 nm with $g_\perp$ = 2.268 and $g_\perp$ = 2.087.[34]
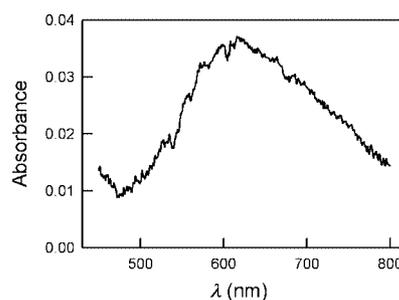

Figure 5. Electronic spectrum of 0.5 mM RU of Cu^{II}-**P1** under the conditions for the oxidative catalysis.

The oxidative catalysis is further investigated with the di-Cu oxidase specific inhibitor kojic acid (KA) [5-hydroxy-2-(hydroxymethy1)-γ-pyrone] (structure shown in Figure 6a).[35] The α-ketoenolate moiety of KA mimics the catechol group during oxidation. The inhibition of Cu^{II}-**P1** by KA toward THB oxidation in the absence of H$_2$O$_2$ follows a competitive pattern (Figure 6a), with an inhibition constant of K_i = 0.34 mM. KA inhibition of di-Cu enzyme is much more specific, e.g., K_i was found to be 3.4 μM toward *Streptomyces antibioticus* tyrosinase[36] and the IC$_{50}$ is 0.28 mM toward lobster polyphenol oxidase with catechol as the substrate,[35c] and the inhibition toward several polyphenol oxidases from various sources exhibit a competitive or a mixed pattern with K_i values in a range of 0.02 to 0.7 mM.[35b]
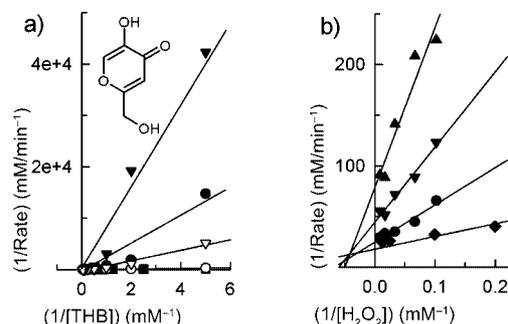
Figure 6. a) Kojic acid (with the structure shown as inset) inhibition (from bottom, 0, 0.5, 2.0, 3.0, 6.0 mM) toward THB oxidation by 10 μM Cu^{II}-**P1** at 100 mM H_2O_2 in 0.1 M MES buffer-methanol solution, showing a competitive inhibition pattern. b) Inhibition of THB oxidation (2.0 mM) by kojic acid (from bottom, 0, 0.5, 1.0, 2.0 mM) at varying amounts of $[H_2O_2]$, showing a mixed inhibition pattern against H_2O_2.

Conversely, the inhibition of KA toward THB oxidation as a function of $[H_2O_2]$ exhibits *a mixed pattern* (Figure 6b) and close to a non-competitive pattern with inhibition constants of $K_{ic} = 4.2$ mM and $K_{iu} = 5.9$ mM, for the dissociation of KA from the ternary complexes KA-(THB-Cu^{II}-**P1**) and KA-(THB/H_2O_2-Cu^{II}-**P1**), respectively. The mixed inhibition pattern indicates that KA and H_2O_2 are not completely exclusive, which also reflect that the binding natures of the substrate and H_2O_2 may be different (however, their bindings to the metal center are observed herein to affect each other; Figure 2). The inhibition results suggest that Cu^{II}-**P1** catalysis has catechol/polyphenol oxidase characteristics and is likely to follow a dinuclear mechanism for the 2-electron oxidation reaction of catechol and polyphenol as the enzymes.

Proposed Mechanism and Modeling

The 2-electron oxidation catalyses herein with and without H_2O_2 are consistent with the mechanism of dinuclear catechol oxidase.[6,41] A random bi-substrate mechanism is proposed (Figure 7) based on the kinetic studies described herein and according to the catalytic pathways of catechol oxidase. In the absence of H_2O_2, THB is bound to and oxidized by Cu^{II}-**P1** (●; Figure 1a) in form of a dinuclear Cu^{II} center by inner-sphere 2-electron transfer to yield Cu^{I}_2 and *o*-quinone product (steps **A**, **B**). The dinuclear center can be formed from two Cu^{II} centers on the same polymer chain separated by three RU or on different polymer chains. The inner-sphere electron transfer is followed by dioxygen binding (**C**) to form a dinuclear Cu^{II}-peroxo center or its isoelectronic forms[3,4] which can also be formed upon peroxide binding (**D** and Figure 1b) analogous to the peroxide shunt pathway in cytochrome P450 mechanism.[37] THB can bind to the dinuclear active site through two pathways (**D**–**G** and **A**, **H**, **G**) and oxidized by the dinuclear Cu^{II}-peroxo center to complete the catalytic cycle. Under reduction conditions, the Cu^{II}-peroxo intermediate is expected to undergo through the pathway **I** to produce H_2O_2 as previously ob-

served.[38] The results presented herein suggest that a dinuclear active center seems to assemble in Cu^{II}-**P1** to afford the high oxidative activity, despite the nature of structural and conformational randomness of copolymers.
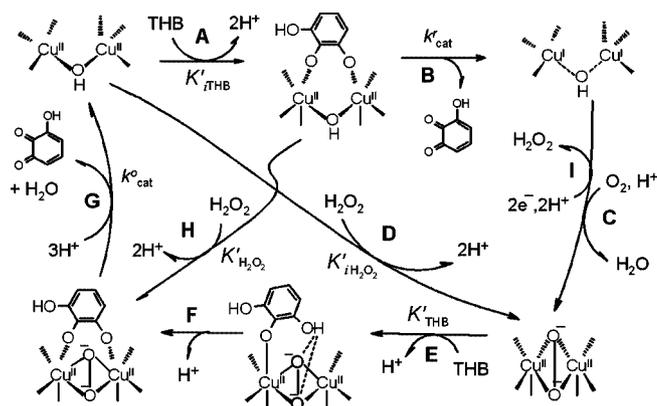

Figure 7. Proposed random bi-substrate mechanism for the oxidation of THB by Cu^{II}-**P1** in the presence (steps **D**–**G** or **A**,**H**,**G**) and absence (**A**–**C** and **E**–**G**) of H_2O_2. The production of H_2O_2 under reduction conditions (**I**) is also consistent with this mechanism. The substrate complexes at steps **E** and **F** are also shown in Figure 4. The kinetic parameters can be obtained from the secondary plots of the Hanes equation.

The sequence and structure of a copolymer chain is random in nature and best described in terms of RU. The coordination sphere of Cu^{II}-**P1** is explored with molecular mechanics calculations (MM3 force field,[39] BioCACHe 6.0, Fujitsu, Beaverton, OR), which reveal that the best coordination sphere is formed by pyridine ligands from different RUs, i.e., pyridines separated by more than 3 monomeric units. Metal binding to pyridines from the same RU of $4Vp_3Ac_1$ causes significant distortion of metal–pyridine coordination. Metal binding to pyridines from different polymer chains afford a more preferred binding mode (≈ 400 kcal/mol lower), which can result in crosslink of the polymer chains and coagulation of the metallopolymer complexes at higher concentrations as we observed previously.[17] The complex is soluble under the conditions herein for kinetic studies.

Because the results from the kinetic studies are consistent with a dinuclear catalysis, the active oxygenated intermediate is modeled with a dinuclear center analogous to that of hemocyanin with a pseudo-C_{2h} symmetry[40] (Figure 8a). This oxy/peroxy dinuclear site allows substrate binding to one of the metal ions from the top or bottom of the Cu–O_2–Cu plane without distorting the overall coordination sphere. A catechol substrate can be docked into the dinuclear site of peroxide-bound Cu^{II}-**P1** without significant distortion (Figure 8b), in which catechol is bound to one Cu center through a deprotonated hydroxy while the other hydroxy forms a H-bond with the bridging peroxide and a proximal amide group from the polymer. Upon deprotonation and binding of the second hydroxy group to the other Cu center (Figure 8c), the energy is lowered relatively by ca.

240 kcal/mol. This binding mode has been suggested to be the case in the enzyme-substrate complex of catechol oxidase.[6,41] However, the coordination is significantly distorted from the original, in which the Cu–O$_2$–Cu plane is puckered to the opposite direction.
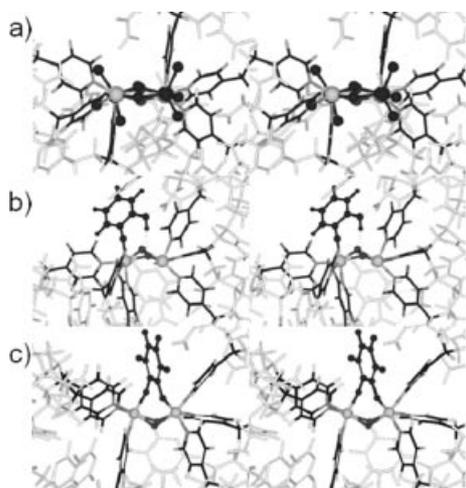

Figure 8. Stereo plots of a) Coordination structure of a putative dinuclear site in Cu^II-**P1** calculated with the MM3 force field protocol. The di-copper site in hemocyanin (dark ball-and-stick) is superimposed onto the structure to show their similarity. The Cu ions are shown as gray spheres and the bridging peroxo as dark spheres. b) Docking of catechol (dark ball and stick) to the dinuclear site of Cu^II-**P1** reveals a favorable binding configuration, in which catechol is bound to one Cu^II through a deprotonated hydroxy while the other hydroxy is still protonated and H-bonding with the bridging peroxide and a proximal amide group from the polymer. c) Catechol is bound to the two metal ions upon deprotonation of the second hydroxy group, which causes distortion of the di-Cu^II center.

Oxidative Plasmid DNA Cleavage

Cu^II-**P1** shows a significant activity toward oxidative cleavage of plasmid DNA which displays unique reaction features. Both the activity and the DNA cleavage pattern by the complex are different from bare Cu^II ions (Figure 9), wherein nicking of the supercoiled (*sc*) plasmid by 50 μM RU of Cu^II-**P1** rapidly occurs within 10 min (lane **1**) to yield both nicked circular (*nc*) and linear (*ln*) forms of the plasmid. The *nc* form can also be cleaved into *ln* form, but still retains a significant amount after two hours (lane **6**). The *nc* form shows a pseudo-first-order decay with a rate constant $k_1 = 0.0095$ min^{-1} (●, Figure 9), suggesting possible double-stranded (ds) cleavage of the *nc* form to yield the *ln* form in a single step. However, the formation of the *ln* form follows a bi-exponential kinetics (▲, Figure 9), which can be deconvoluted into a fast initial increase with a pseudo-first-order rate constant 0.066 min^{-1} in the first 20 min and a slower rate with a pseudo-first-order rate constant the same as that for the decay of the *nc* form (0.0095 min^{-1}). The former is probably also partially attributed to the cleavage of the *sc* form. The initial concentration of the *nc* form is slightly greater than the final concentration of the *ln* form.

This difference suggests that additional pathway(s) may be present for the disappearance of the *ln* form, such as further cleavage to yield small fragments that cannot be revealed on the gel.
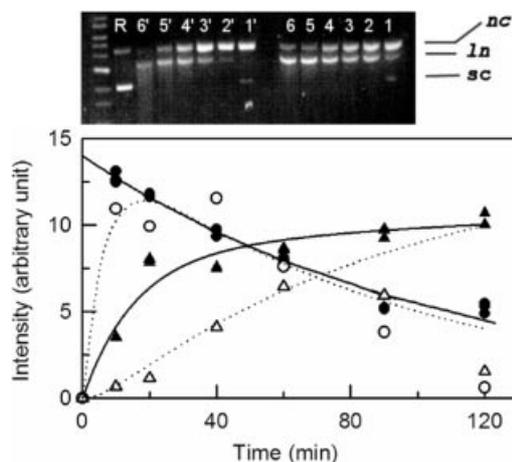

Figure 9. Time course (10, 20, 40, 60, 90, 120 min, lanes **1**–**6** and **1′**–**6′**, respectively) of plasmid cleavage by Cu^II-**P1** in the presence of 1.0% H$_2$O$_2$ (lanes **1**–**6**, 50.0 μM RU; ●, *nc* form; ▲, *ln* form; and theoretical fittings, solid traces) and by free Cu^II/H$_2$O$_2$ (50 μM, lanes **1′**–**6′**; o, *nc* form; Δ, *ln* form; and theoretical fitting, dotted traces) at pH 8.0 and room temperature, stained with ethidium bromide. The standard DNA ladder starts with 1 kbp from the bottom with 1 kbp increment upward. **R** is the plasmid DNA pQE30Xa of ca. 3.5 kbp without treatment. The data are fitted with the kinetic models discussed in the text.

Cu^II ions can cleave plasmids in the presence of an oxidation agent,[42] thus serve as the reference herein (lanes **1′**–**6′**). Under the same conditions, Cu^II cleaves the *sc* and *nc* forms into *ln* form less effectively than Cu^II-**P1**. The *ln* form is not apparent until about 20 min later (lane **2′**), resulting in accumulation of the *nc* form. The buildup of *nc* concentration (due to single-stranded ss-DNA cleavage) and slow appearance of *ln* (due to ds-DNA cleavage) is consistent with a random ss cleavage in which about 1% ds cleavage is expected statistically for every ss cleavage.[43] A simultaneous fitting of the time-dependent changes of both *nc* and *ln* forms to a consecutive kinetic pattern, i.e., *sc*→*nc*→*ln* reveals that the formation of *nc* and *ln* forms up to 60 min can be reasonably fitted (dotted traces, Figure 9) without considering ds cleavage of the *sc* form (however, the disappearance of the *sc* form cannot be clearly traced within the time frame). A drastic change after 60 min (lanes **4′**–**6′**) on both forms may reflect their quick degradation due to random multiple-site nicking to yield small fragments as shown by the smeared gel pattern.

The results reveal that Cu^II-**P1** shows an apparent preference toward nicking and cleavage of *sc* ds-DNA (to afford *nc* and *ln* forms, respectively) as well as cleaving *nc* form into *ln* form, rather than random cleavage toward all forms of plasmid as in the case of DNA cleavage by hydroxy radicals which cannot be described by the kinetic patterns herein. The cleavage pattern by Cu^II-**P1** is reminiscent of

Cu^{II}-bleomycin[44] and a few chemical model systems[45] that have been demonstrated to exhibit ds-DNA cleavage. The apparent ds-DNA cleavage activity of Cu^{II}-**P1** may be attributed to that this macromolecular complex does not quickly diffuse away from the reaction site after one DNA strand is cleaved due to its large size and a possible involvement of H-bonding interaction between the complex and DNA. As a consequence, subsequent cleavage of the second strand can proceed effectively and become apparent in the early stage of the reaction (lanes **1** and **2**). Moreover, the local Cu^{II} concentration in Cu^{II}-**P1** is high which may result in localized cleavage. Herein, the plasmid shows no observable migration retardation in the gel that can be justified to be attributable to interaction with the metallopolymer. If there is any, it must be transient during the fast reaction which cannot be revealed with the gel method. The copolymer itself and H_2O_2 separately did not exhibit noticeable effect on the plasmid in two hours under the same conditions.

The oxidative DNA cleavage by this metallopolymer is quite effective compared to other systems.[46–48] For instance, linearization and further cleavage of plasmid DNA was observed in 30 min by a dinuclear Cu^{II} complex of 5 μM in the presence of 3-mercapto-propionic acid, while only partial nicking of *sc* plasmid was observed by a mononuclear Cu^{II} complex under the same conditions;[46] supercoiled plasmid was nicked by 20-μg Cu^{II}-polymer complex in 10 min in the presence of monoperoxyphthalate;[47] linearization of plasmid DNA by 10-μM Cu^{II} in the presence of 25-μM 2-*tert*-butyl 1,4-hydroquinone was reported to occur in 30 min.[48] The results show that Cu^{II}-**P1** can serve as an efficient and selective "artificial DNase" toward the cleavage of *sc* and *nc* ds-DNA. Since ds-DNA cleavage is a key to trigger cell apoptosis,[14b] the observation of the ds-DNase activity of Cu^{II}-**P1** points a direction for rational design of DNA-targeting drugs for therapeutic purposes, e.g., clustered redox-metal centers with a high local metal concentration to afford a high ds-DNase activity.

Conclusions

Oxidation catalysis by the metallopolymer Cu^{II}-**P1** in the presence of the green oxidation agents H_2O_2 and/or air toward the oxidation of catechol/polyphenol and DNA cleavage is quite proficient. Moreover, the presence of cooperative catalysis by Cu^{II}-**P1** is also very unique among chemical systems. Despite the fact that polymers are considered mostly unstructured, the "active center" in metallopolymers herein seems to be able to assemble into a dinuclear site to exhibit a significant catechol oxidase-like 2-electron oxidative activity toward polyphenol and catechol. Linear copolymers with specifically designed side chains have recently been demonstrated to exhibit high affinities toward target proteins with association constant in the order of 10^5–10^7 M^{-1},[49] wherein the "induced-fit" theory has been suggested to play a role in the recognition of the target prot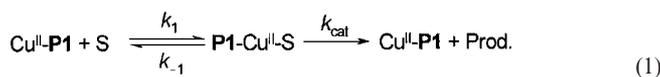eins by the flexible linear copolymers. Such enzyme-like phenomenon may also play a role in catalysis associated with the flexible chains of Cu^{II}-**P1** which can form H-bonding via its amide groups. The easy synthesis of **P1** and its metal complexes suggests that it can serve as a template for further design of metallopolymer systems for various chemical, biological, and environmental applications.[50]

Experimental Section

All the chemicals in this report are commercially available. The synthesis of the copolymer **P1** follows the literature procedures.[17,51] The formation of the polymer and its RU stoichiometry are confirmed with ^1H NMR, wherein the spectrum of the polymer exhibit broad signals as reported which are distinct from the sharp features from the monomers.[17] Electronic spectra of the samples <1.0 mM prepared with $Cu(CH_3COO^-)_2$ and the polymer in aqueous methanol solution were obtained with a Varian Cary50 spectrophotometer. Electron paramagnetic resonance (EPR) experiments were performed with a Bruker Elexsys E580 cw/pulsed X-band spectrometer. For a typical cw EPR spectrum at ca. 5–6 K, the field was set wide enough to reveal a possible low-field transition for magnetically coupled systems with a microwave frequency of 9.4 GHz, field modulation typically around 2 G, and time constant of 40–80 ms. The *g* and *A* tensors were obtained with numerical fitting program provided by Bruker.

The initial rates of the oxidation of catechol and analogs by 10-μM Cu^{II}-**P1**(RU) in buffered aqueous methanol solution (50%) at pH 6.0 with fixed amounts of H_2O_2 were determined with a Varian Cary50 spectrophotometer. The oxidation of the polyphenol 1,2,3-trihydroxybenzene (THB) can be directly monitored at 420 nm (ε = 4583 M^{-1} cm^{-1}) and DTBC 420 nm (ε = 1910 M^{-1} cm^{-1}).[52] Alternatively, 3-methyl-2-benzothiazolinone hydrazone (MBTH) can trap *o*-quinone to form a red adduct (ε_{500} = 3.25 × 10^4 M^{-1} cm^{-1}).[53]

Pre-equilibrium kinetics can be described as the binding of a substrate to the catalytic metal center to form an intermediate **P1**-Cu^{II}-S complex, followed by the conversion of the bound substrate into products [Equation (1)]. The rate law for this reaction mechanism is expressed as in Equation (2), with $K' = (k_{-1} + k_{cat})/k_1$ as the apparent dissociation constant of the **P1**-Cu^{II}-S complex, assuming that the concentration of the complex is much lower than that of unbound substrate. Herein, the initial rates for the oxidation of a catechol substrate S at different concentrations are determined and fitted to Equation (2) to yield the rate constant k_{cat} and K'.

$$Cu^{II}\text{-}P1 + S \underset{k_{-1}}{\overset{k_1}{\rightleftharpoons}} P1\text{-}Cu^{II}\text{-}S \xrightarrow{k_{cat}} Cu^{II}\text{-}P1 + \text{Prod.} \qquad (1)$$

$$rate = \frac{k_{cat}[Cu^{II}\text{-}P1][S]}{K' + [S]} \qquad (2)$$

For a random bi-substrate reaction, the rate of catalysis of one substrate S1 is systematically determined at various concentrations of the other substrate S2 (i.e., rate vs. [S1] at various [S2]) and the data analyzed by the use of the Hanes plots [Equation (3)], wherein A can be fixed to either S1 or S2 and B is the other variable once A is fixed.[28]

$$\frac{[A]}{v_0} = \frac{(1 + K'_B/[B])}{V_{max}}[A] + \frac{K'_A}{V_{max}}\left(1 + \frac{K'_{iA} K'_B}{[B]K'_A}\right) \tag{3}$$

K'_A and K'_B are apparent dissociation constants for the virtual dissociation of A and B, respectively, of the ternary complex with both A and B bound to the catalytic center and K'_{iA} the intrinsic dissociation constant for A from its bound form. The secondary plots of the slope $(1 + K'_B/[B])/V_{max}$ and the y-intercept $(K'_A/V_{max})(1 + K'_{iA} K'_B/[B]K'_A)$ from the Hanes plot [Equation (3)] yield the dissociation constants. Inhibitions were carried in a similar fashion as the kinetic measurement, but in the presence of different amounts of inhibitors to establish the inhibition patterns.

The activity of Cu^{II}-P1 toward DNA cleavage was determined by incubating 50.0 μM of Cu^{II}-P1(RU) with 0.15 μg pQE30Xa plasmid (Quiagen) in the presence of 1.0% H$_2$O$_2$ buffered with 50-mM HEPES at pH 8.0 in a volume of 12.0 μL at different time periods. The oxidative cleavage of plasmid DNA was detected with 1% agarose gel electrophoresis (150 V, 1× Tris-acetate buffer for one hour). All plastic ware was demetallized with EDTA and rinsed with 18 MΩ water.

Acknowledgments

[1] a) M. Jaiswal, R. Menon, *Polym. Inter.* **2006**, *55*, 1371–1384; b) A. L. Stepanov, R. I. Khaibullin, *Rev. Adv. Mater. Sci.* **2004**, *7*, 108–125.

[2] J. Suh, *Acc. Chem. Res.* **2003**, *36*, 562–570.

[3] a) K. D. Karlin, A. D. Zuberbühler in *Bioinorganic Catalysis: Second Edition* (Eds.: J. Reedijk, E. Bouman), Marcel Dekker, New York, **1999**, 469–534; b) L. Q. Hatcher, K. D. Karlin, *J. Biol. Inorg. Chem.* **2004**, *9*, 669–683.

[4] a) E. A. Lewis, W. B. Tolman, *Chem. Rev.* **2004**, *104*, 1047–1076; b) N. Kitajima, Y. Moro-oka, *Chem. Rev.* **1994**, *94*, 737–757.

[5] I. Bertini, H. B. Gray, S. J. Lippard, J. S. Valentine (Eds.), *Bioinorganic Chemistry*, University Science Books, Sausalito, CA, **1994**.

[6] E. I. Solomon, U. M. Sundaram, T. E. Machonkin, *Chem. Rev.* **1996**, *96*, 2563–2605.

[7] C. Chen, L. Milne, R. Landgraf, D. M. Perrin, D. S. Sigman, *ChemBioChem* **2001**, *2*, 735–740.

[8] D. S. Sigman, *Biochemistry* **1990**, *29*, 9097–9105.

[9] M. A. Kopf, K. D. Karlin in *Biomimetic Oxidations* (Ed.: B. Meunier), Imperial College Press, London, **2000**, ch. 7.

[10] J. P. Klinman, *Chem. Rev.* **1996**, *96*, 2541–2561.

[11] a) T. J. Collins, *Acc. Chem. Res.* **2002**, *35*, 782; b) A. Sorokin, J.-L. Séris, B. Meunier, *Science* **1995**, *268*, 1163–1165; c) P. T. Anastas, M. M. Kirchhoff, *Acc. Chem. Res.* **2002**, *35*, 686–694; d) D. Lenoir, C. Horwitz, K. W. Schramm, T. J. Collins, *Science* **2002**, *296*, 326; e) P. T. Anastas, J. C. Warner, *Green Chemistry: Theory and Practice*, Oxford University Press, Baltimore, **2000**.

[12] E. R. Stadtman, *Ann. N. Y. Acad. Sci.* **2000**, *928*, 22–38.

[13] K. S. Kasprzak, *Free Radical Biol. Med.* **2002**, *32*, 958–967.

[14] a) D. G. Tang, E. H. La, J. Kern, J. P. Kehrer, *Biol. Chem.* **2002**, *383*, 425–442; b) M. Stanulla, J. Wang, D. S. Chervinsky, S. Thandla, P. D. Aplan, *Mol. Cell Biol.* **1997**, *17*, 4070–4079.

[15] J. Chin, *Acc. Chem. Res.* **1991**, *24*, 145–152.

[16] K. D. Karlin, *Science* **1993**, *26*, *261*, 701–708.

[17] A. I. Hanafy, V. Lykourinou-Tibbs, K. S. Bisht, L.-J. Ming, *Inorg. Chim. Acta* **2005**, *358*, 1247–1252.

[18] a) G. R. A. Johnson, N. B. Nazhat, *J. Am. Chem. Soc.* **1987**, *109*, 1990–1994; b) R. Alnaizy, A. Akgerman, *Adv. Environ. Res.* **2000**, *4*, 233–244; c) J. A. Zazo, J. A. Casas, A. F. Mohedano, M. A. Gilarranz, J. J. Rodríguez, *Environ. Sci. Technol.* **2005**, *39*, 9295–9302; d) M. Edalatmanesh, R. Dhib, M. Mehrvar, *Int. J. Chem. Kinet.* **2007**, *40*, 34–43.

[19] For comparison, over-the-counter H$_2$O$_2$ solution for household use in the U. S. is 3%.

[20] N. Sengottuvelan, D. Saravanakumar, V. Narayanan, M. Kandaswamy, K. Chinnakali, G. Senthilkumar, *Bull. Chem. Soc. Jpn.* **2004**, *77*, 1153–1159.

[21] P. Akilan, M. Thirumavalavan, M. Kandaswamy, *Polyhedron* **2003**, *22*, 3483–3492.

[22] S. C. Cheng, H. H. Wei, *Inorg. Chim. Acta* **2002**, *340*, 105–113.

[23] C.-T. Yang, M. Vetrichelvan, X. Yang, B. Moubaraki, K. S. Murray, J. J. Vittal, *Dalton Trans.* **2004**, 113–121.

[24] E. Monzani, L. Quinti, A. Perotti, L. Casella, M. Gullotti, L. Randaccio, S. Geremia, G. Nardin, P. Faleschini, G. Tabbi, *Inorg. Chem.* **1998**, *37*, 553–562.

[25] A. Harada, A. Fukushima, K. Shiotsuki, H. Yamaguchi, F. Oka, M. Kamachi, *Inorg. Chem.* **1997**, *36*, 6099–6102.

[26] a) I. A. Koval, C. Selmeczi, C. Belle, C. Philouze, E. Saint-Aman, I. Gautier-Luneau, A. M. Schuitema, M. van Vliet, P. Gamez, O. Roubeau, M. Lüken, B. Krebs, M. Lutz, A. L. Spek, J.-L. Pierre, J. Reedijk, *Chem. Eur. J.* **2006**, *12*, 6138–6150; b) J. Ackermann, S. Buchler, F. Meyer, *C. R. Chim.* **2007**, *10*, 421–432.

[27] A. Rompel, H. Fischer, D. Meiwes, K. Buëldt-Karentzopoulos, A. Magrini, C. Eicken, C. Gerdemann, B. Krebs, *FEBS Lett.* **1999**, *445*, 103–110.

[28] V. Leskovac, *Comprehensive Enzyme Kinetics*, Kluwer/Plenum, Boston, MA, **2002**, pp. 122–124.

[29] M. Martin, F. Manea, R. Fiammengo, L. J. Prins, L. Pasquato, P. Scrimin, *J. Am. Chem. Soc.* **2007**, *129*, 6982–6983.

[30] J. D. Epperson, L.-J. Ming, G. R. Baker, G. R. Newkome, *J. Am. Chem. Soc.* **2001**, *123*, 8583–8592.

[31] J. Peisach, W. E. Blumberg, *Arch. Biochem. Biophys.* **1974**, *165*, 691–708.

[32] a) S. Torelli, C. Belle, I. Gautier-Luneau, J. L. Pierre, *Inorg. Chem.* **2000**, *39*, 3526–3536; b) C. Belle, C. Beguin, I. Gautier-Luneau, S. Hamman, C. Philouze, J. L. Pierre, F. Thomas, S. Torelli, *Inorg. Chem.* **2002**, *41*, 479; c) C.-H. Lee, S.-T. Wong, T.-S. Lin, C.-Y. Mou, *J. Phys. Chem. B* **2005**, *109*, 775–784.

[33] I. Bertini, E. Borghi, C. Luchinat, *J. Am. Chem. Soc.* **1979**, *101*, 7069–7071.

[34] a) R. J. Carrico, H. F. Deutsch, *J. Biol. Chem.* **1969**, *244*, 6087–6093; b) G. Rotilio, A. F. Agro, L. Calabrese, F. Bossa, P. Guerrieri, B. Mondovi, *Biochemistry* **1971**, *10*, 616–621.

[35] a) R. Saruno, F. Kato, T. Ikeno, *Agric. Biol. Chem.* **1979**, *43*, 1337–1339; b) J. S. Chen, C. Wei, R. S. Rolle, W. S. Otwell, M. O. Balaban, M. R. Marshall, *J. Agric. Food Chem.* **1991**, *39*, 1396–1401; c) J. S. Chen, C.-i. Wei, M. R. Marshall, *J. Agric. Food Chem.* **1991**, *39*, 1897–1901.

[36] L. Bubacco, E. Vijgenboom, C. Gobin, A. W. J. W. Tepper, J. Salgado, G. W. Canters, *J. Mol. Catal. B* **2000**, *8*, 27–35.

[37] M. Sono, M. P. Roach, E. D. Coulter, J. H. Dawson, *Chem. Rev.* **1996**, *96*, 2841–2887.

[38] a) X. Huang, C. S. Atwood, M. A. Hartshorn, G. Multhaup, L. E. Goldstein, R. C. Scarpa, M. P. Cuajungco, D. N. Gray, J. Lim, R. D. Moir, R. E. Tanzi, A. I. Bush, *Biochemistry* **1999**, *38*, 7609–7616; b) I. A. Koval, C. Selmeczi, C. Belle, C. Philouze, E. Saint-Aman, I. Gautier-Luneau, A. M. Schuitema, M. van Vliet, P. Gamez, O. Roubeau, M. Lüken, B. Krebs, M. Lutz, A. L. Spek, J.-L. Pierre, J. Reedijk, *Chem. Eur. J.* **2006**, *12*, 6138–6150; c) K. Born, P. Comba, A. Daubinet, A. Fuchs, H. Wadepohl, *J. Biol. Inorg. Chem.* **2007**, *12*, 36–48.

[39] N. L. Allinger, Y. H. Yuh, J. H. Lii, *J. Am. Chem. Soc.* **1989**, *111*, 8551–8566.

[40] a) B. Hazes, K. A. Magnus, C. Bonaventura, J. Bonaventura, Z. Dauter, K. H. Kalk, W. G. J. Hol, *Prot. Sci.* **1993**, *2*, 597–

619; b) K. A. Magnus, B. Hazes, H. Tonthat, C. Bonaventura, J. Bonaventura, W. G. J. Hol, *Proteins–Struct. Funct. Genet.* **1994**, *19*, 302–309.

[41] A. Rompel, H. Fischer, D. Meiwes, K. Büldt-Karentzopoulos, R. Dillinger, F. Tuczek, H. Witzel, B. Krebs, *J. Biol. Inorg. Chem.* **1999**, *4*, 56–63.

[42] P. Tachon, *Free Radiat. Res. Commun.* **1989**, *7*, 1–10.

[43] a) L. F. Povirk, W. Wübker, W. Köhnlein, F. Hutchinson, *Nucleic Acids Res.* **1977**, *4*, 3573–3580; b) P. U. Maheswari, K. Lappalainen, M. Sfregola, S. Barends, P. Gamez, U. Turpeinen, I. Mutikainen, G. P. van Wezel, J. Reedijk, *Dalton Trans.* **2007**, 3676–3683.

[44] G. M. Ehrenfeld, L. O. Rodriguez, S. M. Hecht, C. Chang, V. J. Basus, N. J. Oppenheimer, *Biochemistry* **1985**, *24*, 81–92.

[45] a) F. V. Pamatong, C. A. Detmer III, J. R. Bocarsly, *J. Am. Chem. Soc.* **1996**, *118*, 5339; b) C. A. Detmer III, F. V. Pamatong, J. R. Bocarsly, *Inorg. Chem.* **1996**, *35*, 6292–6298.

[46] K. J. Humphreys, A. E. Johnson, K. D. Karlin, S. E. Rokita, *J. Biol. Inorg. Chem.* **2002**, *7*, 835–842.

[47] C. Madhavaiah, S. G. Srivatsan, S. Verma, *Catal. Commun.* **2003**, *4*, 237–241.

[48] Y. Li, A. Seacat, P. Kuppusamy, J. L. Zweier, J. D. Yager, M. A. Trush, *Mutat. Res.* **2002**, *518*, 123–133.

[49] S. J. Koch, C. Renner, X. Xie, T. Schrader, *Angew. Chem. Int. Ed.* **2006**, *45*, 6352–6355.

[50] Preliminary results show that phenol can be hydroxylated and oxidized and chlorocatechols oxidized by Cu^{II}-**P1** to yield *o*-quinones. On the design side, the Cu^{II} complex of a 4-vinylpyridine-vinylstyrene copolymer seems to oxidize THB and DTBC with rates higher than Cu^{II}-**P1** under similar conditions described herein.

[51] K. E. Geckler, N. Arsalani, *J. Macromol. Sci., Pure Appl. Chem.* **1996**, *A33*, 1165–1179.

[52] S. Grabiec, W. Tomassi, T. Podbielski, *Bull. L'Acad. Polon. Sci., Ser. Sci. Biol.* **1974**, *22*, 187–191.

[53] a) J. C. Espin, M. Morales, R. Varon, J. Tudela, F. Garcia-Canovas, *Anal. Biochem.* **1995**, *231*, 237; b) J. C. Espin, J. Tudela, F. Garcia-Canovas, *Anal. Biochem.* **1998**, *259*, 118.